

1 Main Manuscript for

2 Constraints on the evolution of toxin-resistant Na,K-ATPases have limited
3 dependence on sequence divergence.

4 Shabnam Mohammadi^{1,2,*}, Santiago Herrera-Álvarez^{4,5,*}, Lu Yang^{3,§,*}, María del Pilar Rodríguez-
5 Ordoñez^{4,#}, Karen Zhang³, Jay F. Storz¹, Susanne Dobler², Andrew J. Crawford⁴ & Peter
6 Andolfatto⁶

7 ¹School of Biological Sciences, University of Nebraska, Lincoln, NE, USA

8 ²Molecular Evolutionary Biology, Institute of Zoology, Universität Hamburg, Hamburg, Germany

9 ³Department of Ecology and Evolution, Princeton University, Princeton, NJ, USA

10 ⁴Department of Biological Sciences, Universidad de los Andes, Bogotá, 111711, Colombia

11 ⁵Department of Ecology and Evolution, University of Chicago, Chicago, IL, USA

12 ⁶Department of Biological Sciences, Columbia University, New York, NY, USA

13

14 *Co-first authorship

15 § Current address: Wellcome Sanger Institute, Cambridge, United Kingdom

16 # Current address: Université Paris-Saclay Evry, Evry, France

17

18 Email: pa2543@columbia.edu

19

20 SM: 0000-0003-3450-6424, LY: 0000-0002-2694-1189, SHA: 0000-0002-0793-7811, MPRO:
21 0000-0002-0856-1297, KZ: 0000-0003-4406-9977, JFS: 0000-0001-5448-7924, SD: 0000-0002-
22 0635-7719, AJC: 0000-0003-3153-6898, PA: 0000-0003-3393-4574

23

24 Classification

25 Biological Sciences; Evolution

26 Keywords

27 Epistasis, protein evolution, cardiotoxic steroids, toxin resistance, adaptation

28 Author Contributions

29 PA and AJC conceived of and oversaw the project; SM, JFS, SD, AJC and PA
30 designed experiments; KZ, LY, MPRO, SHA, SM collected data; SM, SHA and PA
31 performed evolutionary and statistical analyses; SM, SHA, and PA wrote the paper; All authors
32 edited the manuscript.

33 This PDF file includes:

34 Main Text

35 Figures 1 to 6

36

37 **Abstract**

38 A growing body of theoretical and experimental evidence suggests that intramolecular epistasis is
39 a major determinant of rates and patterns of protein evolution and imposes a substantial constraint
40 on the evolution of novel protein functions. Here, we examine the role of intramolecular epistasis
41 in the recurrent evolution of resistance to cardiotonic steroids (CTS) across tetrapods, which occurs
42 via specific amino acid substitutions to the α -subunit family of Na,K-ATPases (ATP1A). After
43 identifying a series of recurrent substitutions at two key sites of ATP1A that are predicted to confer
44 CTS resistance in diverse tetrapods, we then performed protein engineering experiments to test
45 the functional consequences of introducing these substitutions onto divergent species
46 backgrounds. In line with previous results, we find that substitutions at these sites can have
47 substantial background-dependent effects on CTS resistance. Globally, however, these
48 substitutions also have pleiotropic effects that are consistent with additive rather than background-
49 dependent effects. Moreover, the magnitude of a substitution's effect on activity does not depend
50 on the overall extent of ATP1A sequence divergence between species. Our results suggest that
51 epistatic constraints on the evolution of CTS-resistant forms of Na,K-ATPase likely depend on a
52 small number of sites, with little dependence on overall levels of protein divergence. We propose
53 that dependence on a limited number sites may account for the observation of convergent CTS
54 resistance substitutions observed among taxa with highly divergent Na,K-ATPases.

55

56

57 **Significance Statement**

58 Individual amino acid residues within a protein work in concert to produce a functionally coherent
59 structure that must be maintained even as orthologous proteins in different species diverge over
60 time. Given this dependence, we expect identical mutations to have more similar effects on protein
61 function in more closely related species. We tested this hypothesis by performing protein-
62 engineering experiments on ATP1A, an enzyme mediating target-site insensitivity to cardiotonic
63 steroids (CTS) in diverse animals. These experiments reveal that the phenotypic effects of
64 substitutions can sometimes be background-dependent, but also that the magnitude of these
65 phenotypic effects does not correlate with overall levels of ATP1A sequence divergence. Our
66 results suggest that epistatic constraints are determined by states at a small number of sites,
67 potentially explaining the frequent convergent CTS resistance substitutions among Na,K-ATPases
68 of highly divergent taxa.

69 **Main Text**

70

71 **Introduction**

72

73 Instances of parallel and convergent (hereafter “convergent”) evolution represent a useful paradigm
74 to examine the factors that limit the rate of adaptation and the extent to which adaptive evolutionary
75 paths are predictable [1,2]. The evolution of resistance to cardiotoxic steroids (CTS) in animals
76 represents one of the clearest examples of convergent molecular evolution. CTS are potent
77 inhibitors of Na,K-ATPase (NKA, Fig. 1A), a protein that plays a critical role in maintaining
78 membrane potential and is consequently vital for the maintenance of many physiological processes
79 and signaling pathways in animals [3]. CTS inhibit NKA function by binding to a highly conserved
80 domain of the protein’s α -subunit (ATP1A) and blocking the exchange of Na⁺ and K⁺ ions [3]. Thus,
81 NKA is often the target of convergent evolution of CTS resistance across widely divergent species,
82 including insect herbivores that feed on toxic plants [4,5] as well as predators that feed on toxic
83 prey [6–10].

84

85 Patterns of convergence in adaptive protein evolution are influenced by the mutational target size
86 (i.e. the number of potentially adaptive mutations), the degree of pleiotropy (i.e. the effect of a given
87 mutation on multiple phenotypes), and intramolecular epistasis (i.e. nonadditive interactions
88 between mutant sites in the same protein) [11–19]. If the phenotypic and fitness effects of mutations
89 depend on the protein sequence background on which they arise (i.e. there is intramolecular
90 epistasis), a given mutation is expected to have more similar phenotypic and fitness effects in
91 orthologs from closely-related species. Therefore, the probability of convergent substitution is
92 expected to decrease with increasing sequence divergence between orthologous proteins in
93 different species. Consistent with this expectation, such a decline is observed in broad-scale
94 phylogenetic comparisons of mitochondrial [20] and nuclear [21,22] proteins. While these results
95 suggest epistasis is an important global determinant of patterns of convergent protein evolution,
96 studies linking these broad-scale observations with functional data at the level of individual proteins
97 are lacking.

98

99 Functional investigations of CTS resistance-conferring substitutions at two key sites (111 and 122)
100 in ATP1A orthologs of *Drosophila* [23,24] and Neotropical grass frogs [25] revealed associated
101 negative pleiotropic effects on protein function and showed that evolution at other sites in the
102 protein mitigate these detrimental effects. In light of these pleiotropic and epistatic constraints, it is
103 curious that convergent CTS-resistant substitutions are often observed among ATP1A orthologs of
104 highly divergent species. Due to limited comparative functional data, the generality of pleiotropic

105 and epistatic constraints on ATP1A-mediated CTS resistance, and specifically the predicted
106 dependence on evolutionary distance, remain poorly understood.

107

108 To achieve a clearer picture of the phylogenetic distribution of CTS resistance substitutions, a more
109 complete and consistent sampling of ATP1A is needed in vertebrates. Broad phylogenetic
110 comparisons in vertebrates have primarily focused on the H1-H2 extracellular loop of ATP1A, which
111 represents only a subset of the CTS-binding domain. Further, most vertebrates possess three
112 paralogs of ATP1A that have different tissue-specific expression profiles and are associated with
113 distinct physiological roles (Fig. 1B) [3,26]. Previous studies of the ATP1A paralogs of vertebrate
114 taxa focused on ATP1A3 in reptiles [7,8,27,28], ATP1A1 and/or ATP1A2 in birds and mammals
115 [10,28], and either ATP1A1 or ATP1A3 in amphibians [6,28]. We therefore lack a comprehensive
116 and systematic survey of amino acid variation in the ATP1A protein family across vertebrates.

117

118 To bridge this gap, we first surveyed variation in near full-length coding sequences of the three
119 NKA α -subunit paralogs (ATP1A1, ATP1A2, ATP1A3) that are shared across major extant tetrapod
120 groups (mammals, birds, non-avian reptiles, and amphibians), and identified substitutions that
121 occur repeatedly among divergent lineages. If the phenotypic effects of these substitutions depend
122 on states at a large number of sites throughout the protein, we expect that identical substitutions
123 should have increasingly distinct effects on more highly divergent proteins. Focusing on two key
124 sites implicated in CTS resistance across animals (111 and 122), we tested whether substitutions
125 at these sites have increasingly distinct phenotypic effects on more divergent genetic backgrounds.
126 We engineered several common substitutions at sites 111 and 122 of ATP1A1 that differ between
127 species to reveal potential 'cryptic' epistasis [16,29]. By quantifying the level of CTS resistance
128 conferred by these substitutions on different backgrounds, as well as their pleiotropic effects on
129 enzyme function, we evaluate the extent to which overall protein sequence background has
130 constrained the evolution of CTS-resistant forms of ATP1A1 across tetrapods.

131

132

133 **Results**

134

135 **Patterns of ATP1A sequence evolution across species and paralogs.**

136

137 To obtain a more comprehensive portrait of ATP1A amino acid variation among tetrapods, we
138 created multiple sequence alignments for near full-length ATP1A proteins for the three ATP1A
139 paralogs shared among vertebrates. In addition to publicly available data, we generated new RNA-
140 seq data for 27 non-avian reptiles (PRJNA754197) (Table S1-S2). We then *de novo* assembled

141 full-length transcripts of all ATP1A paralogs using these and generated new RNA-seq data for 18
142 anuran species [25] (PRJNA627222) to achieve better representation for these groups. In total, this
143 dataset comprises 429 species for ATP1A1, 197 species for ATP1A2 and 204 species for ATP1A3
144 (831 sequences total, including the newly generated data; Supplemental Dataset 1, Fig. S1).

145

146 Our survey reveals numerous substitutions at sites implicated in CTS resistance of NKA (Fig. 2;
147 Supplementary Dataset 2; for comparison to insects, see Supplemental file 1 of ref. [23]). As
148 anticipated from studies of full-length sequences in insects [4,5,23], most amino acid variation
149 among species and paralogs is concentrated in the H1-H2 extracellular loop (residues 111-122;
150 Fig 1A). Despite harboring just 28% of 43 sites previously implicated in CTS resistance [30], the
151 H1-H2 extracellular loop contains 81.4% of all substitutions identified among the three ATP1A
152 paralogs (Fig. S2).

153 Our survey reveals several clade- and paralog-specific patterns. Notably, ATP1A1 exhibits more
154 variation among species at sites implicated in CTS resistance (Fig. 2). Most of the variation in
155 ATP1A2 at these sites is restricted to squamate reptiles and ATP1A3 lacks substitutions at site 122
156 altogether, despite the well-known potential for substitutions at this site to confer CTS resistance
157 [25,31]. Looking across species and paralogs, the extent of convergence at sites 111 and 122 is
158 remarkable (Figs. 2-3): for example, the substitutions Q111E, Q111T, Q111H, Q111L, and Q111V
159 all occur in parallel in multiple species of both insects and vertebrates. N122H and N122D also
160 frequently occur in parallel in both of these major clades. The frequent convergence of CTS-
161 sensitive (i.e. Q111 and N122) to CTS-resistant states at these sites has been interpreted as
162 evidence for adaptive significance of these substitutions [4–7], but may also reflect mutational
163 biases [32] and the nature of physico-chemico constraints [21,33].

164 In contrast, some convergence is restricted to specific clades: for example, Q111R occurs in
165 parallel across tetrapods but has not been observed in insects. Similarly, the combination
166 Q111R+N122D has evolved three times independently in ATP1A1 of tetrapods but is not observed
167 in insects. Conversely, insects have evolved Q111V+N122H independently four times, but this
168 combination has never been observed in tetrapods. These patterns suggest that the fitness effects
169 of some CTS-resistant substitutions depend on genetic background (i.e. epistatic constraints), with
170 the result that CTS-resistance evolved via different mutational pathways in different lineages.

171 Beyond known CTS-resistant substitutions at sites 111 and 122, some taxa have evolved other
172 paths to CTS resistance. For example, horned frogs of the genus *Ceratophrys* are known to prey
173 on CTS-containing toads [34] and their ATP1A1 harbors a known CTS-resistant substitution at site
174 121 (D121N, Supplementary Dataset 2). This substitution is rare among vertebrates but has been

175 previously reported in CTS-adapted milkweed bugs [4,5]. Similarly, the known CTS resistance
176 substitution C104Y is observed in ATP1A1 among garter snakes of the genus *Thamnophis*
177 (Supplementary Dataset 2) and CTS-adapted milkweed weevils [5]. Histicognathi rodents,
178 including Chinchilla (*Chinchilla lanigera*), and yellow-throated sandgrouse (*Pterocles gutturalis*)
179 show distinct single-amino acid insertions in the H1–H2 extracellular loop, a characteristic that has
180 been previously associated with CTS resistance in pyrgomorphid grasshoppers [30,35]. Further, *in*
181 *lieu* of variation at site 122, ATP1A3 of tetrapods harbors frequent convergent substitutions at site
182 120 (G120R, see also [7]). Interestingly, this site also shows substantial convergent substitution in
183 the ATP1A1 paralog of birds (where N120K occurs eight times independently) but is mostly
184 invariant in ATP1A1 of other tetrapods.

185

186 **Context-dependent CTS resistance of substitutions at sites 111 and 122**

187

188 The clade- and paralog-specific patterns of substitution among ATP1A paralogs outlined above
189 suggest that the evolution of CTS resistance may be highly dependent on sequence context.
190 However, the functional effects of the vast majority of these substitutions on the diverse genetic
191 backgrounds in which they occur remain largely unknown [25,27,31]. Given the diversity and broad
192 phylogenetic distribution of convergent substitutions at sites 111 and 122, and the documented
193 effects of some of these substitutions on CTS resistance, we experimentally tested the extent to
194 which functional effects of substitutions at these sites are background-dependent.

195

196 We focused functional experiments on ATP1A1, because it is the most ubiquitously expressed
197 paralog and exhibits both the most sequence diversity and the broadest phylogenetic distribution
198 of convergent substitutions. Specifically, we considered ATP1A1 orthologs from nine
199 representative tetrapod species that possess different combinations of wild-type amino acids at
200 111 and 122 (Fig. 4A). Our taxon sampling included two lizards, two snakes, two birds, two
201 mammals, and previously published data for one amphibian (Fig. S6; Fig. S7; Table S3). The
202 ancestral amino acid states of sites 111 and 122 in tetrapods are Q and N, respectively. We found
203 that the sum of the number of derived states at positions 111 and 122 is a strong predictor of the
204 level of CTS-resistance (Fig 4B, IC_{50} , Spearman's $r_s=0.85$, $p=0.001$). Nonetheless, we also found
205 greater than 10-fold variation in CTS resistance among enzymes that had identical paired states at
206 111 and 122 (e.g., compare chinchilla (CHI) versus red-necked keelback snake (KEE) or compare
207 rat (RAT) versus the resistant paralog of grass frog (GRA_R)). These differences suggest that
208 substitutions at other sites also contribute to CTS resistance.

209

210 To test for epistatic effects of common CTS-resistant substitutions at sites 111 and 122, we used
211 site-directed mutagenesis to introduce 15 substitutions (nine at position 111 and six at position 122)
212 in the wild-type ATP1A1 backgrounds of nine species (Fig. S6). The specific substitutions chosen
213 were either phylogenetically broadly-distributed convergent substitutions and/or divergent
214 substitutions that distinguish closely related clades of species. We expressed each of these 24
215 ATP1A1 constructs with an appropriate species-specific ATP1B1 protein (Table S3). For each
216 recombinant NKA protein complex, we characterized its level of CTS resistance (IC_{50}) and
217 estimated enzyme activity as the rate of ATP hydrolysis in the absence of CTS (Table S4).

218
219 Among the 12 cases for which IC_{50} could be measured, substitutions had a 15-fold effect on
220 average (Fig. 4C, Table S4) and were equally likely to increase or decrease IC_{50} . To assess the
221 background dependence of specific substitutions, we examined five cases in which a given
222 substitution (e.g., E111H), or the reverse substitution (e.g., H111E), could be evaluated on two or
223 more backgrounds. In the absence of intramolecular epistasis, the effect of a substitution on
224 different backgrounds should remain unchanged and the magnitude of the effect of the reverse
225 substitution should also be the same but with opposite sign. This analysis revealed substantial
226 background dependence for IC_{50} in two of the five informative cases (Fig. 4E; Table S5). In one
227 case, the N122D substitution resulted in a 200-fold larger increase in IC_{50} when added to the
228 chinchilla (CHI) background compared to the grass frog (GRA) background ($p=1.2e-3$ by ANOVA).
229 In the other case, the E111H substitution and the reverse substitution (H111E) produced effects in
230 the same direction (reducing CTS-resistance) when added to different backgrounds (false fer-de-
231 lance (FER) and red-necked keelback (KEE) snakes, respectively, $p=1e-7$ by ANOVA). Overall,
232 these results suggest that the effect of a given substitution on IC_{50} can be strongly dependent on
233 the background on which it occurs. The remaining three substitutions (H111T, Q111R and H122D)
234 showed no significant change in the magnitude of the effect on IC_{50} when introduced into different
235 species' backgrounds. These results suggest that, while some substitutions can have strong
236 background-dependent effects, strong intramolecular epistasis with respect to CTS resistance is
237 not universal.

238

239 **Pleiotropic effects on NKA activity largely depend on states at a small set of sites.**

240

241 We next tested whether substitutions at sites 111 and 122 have pleiotropic effects on ATPase
242 activity. Because ion transport across the membrane is a primary function of NKA and its disruption
243 can have severe pathological effects [36], mutations that compromise this function are likely to be
244 under strong purifying selection. As suggested by previous work [23–25], CTS-resistant
245 substitutions at sites 111 and 122 can decrease enzyme activity. We evaluated the generality of

246 these effects across a broader phylogenetic scale by comparing enzyme activity of the 15 mutant
247 NKA proteins to their corresponding wild-type proteins.

248

249 Interestingly, the wild-type enzymes themselves exhibit substantial variation in activity, from 3-18
250 nmol/mg*min ($p=6e-7$ by ANOVA, Fig 4E; Table S4). On average, substitutions at sites 111 and
251 122 on divergent orthologous protein backgrounds changed enzyme activity by 60% (mean of the
252 absolute change; Fig 4D; Fig S4). In two cases, amino acid substitutions at position 122 (N122H
253 and H122D) nearly inactivated lizard NKAs and, in one case, a substitution at position 111 (Q111T)
254 resulted in low expression of the recombinant protein in the transfected cells (Fig S7; Fig. S8). A
255 test of uniformity of pairwise t-test p-values across substitutions suggests a significant enrichment
256 of low p-values (Fig 4D inset; $p=2.5e-4$, chi-squared test of uniformity). Thus, globally, this set of
257 substitutions has significant effects on NKA activity, but they were surprisingly not more likely to
258 decrease than increase activity (10 decrease : 5 increase, $p>0.3$, binomial test, Fig. 4D, Table S5).

259

260 We next asked to what extent pleiotropic effects of CTS resistant substitutions at positions 111 and
261 122 are dependent on genetic background. This question is motivated by recent studies in insects
262 which revealed that deleterious pleiotropic effects of some resistance-conferring substitutions at
263 sites 111 and 122 are background dependent [23,24]. Likewise, recent work on ATP1A1 of toad-
264 eating grass frogs showed that effects of Q111R and N122D on NKA activity are also background
265 dependent [25]. In contrast, among the five informative cases in which we compared the same
266 substitution (or the reverse substitution) on two or more backgrounds, there is no evidence for
267 background dependence (Fig 4E; Table S5). For example, N122D has similar effects on NKA
268 activity in grass frog and chinchilla despite the substantial divergence between the species' proteins
269 (8.4% protein sequence divergence; Fig. 4D). Similarly, the effects of Q111R in ostrich or the
270 reverse substitution R111Q in sandgrouse were not significantly different from the effect of Q111R
271 in grass frog (7.5% and 8% protein sequence divergence, respectively).

272

273 To further examine the evidence for background dependence, we tested whether changes to the
274 same amino acid state (regardless of starting state) at 111 and 122 produce different changes in
275 NKA activity (e.g., R111E on the rat background versus H111E on the false fer-de-lance
276 background). If epistasis is prevalent, involving a large number of sites, we expect that the absolute
277 difference in effects of substitutions to a given amino acid state should increase with increasing
278 sequence divergence of the wild-type ATP1A1 proteins. The 11 possible comparisons reveal
279 substantial variation in the absolute difference of effects on protein activity, ranging from 8% to
280 190% (Table S7). Despite this, we found no relationship between the difference in the effect of
281 substitutions to the same state and the extent of amino acid divergence between the orthologous

282 proteins (Fig. 5A). This pattern suggests that, while pleiotropic effects may be pervasive and can
283 be background dependent [23,25], these effects do not correlate with overall sequence divergence.

284

285 We hypothesized that background-dependent effects may instead depend on states at a small
286 number of sites. If so, using total divergence may obscure a relationship between functional effects
287 and divergence at these sites. To test this hypothesis, we used an analysis of variance to ask which
288 variant sites across our functional constructs best accounted for differences in effects on different
289 backgrounds (Methods and Fig. S5). Of 24 groups of variant sites (grouped as those with Pearson's
290 $r > 0.8$), we discovered two groups that included 16 of 113 total variant sites. These two groups of
291 16 sites jointly accounted for 78% of the variance among construct comparisons ($p < 0.004$ by
292 permutation). Further, in contrast to the pattern observed using all variant sites (Fig. 5A), we found
293 a strong positive correlation between the difference in the effect of substitutions and the extent of
294 divergence at these 16 sites (Fig. 5B; Pearson's $r = 0.78$, $p = 0.003$ by permutation). This analysis
295 strongly supports the notion that background-dependent effects depend on a circumscribed
296 number of sites. While our resolution is limited (due to the limited number of genetic backgrounds
297 in the experiments), we can say that 16 sites or fewer explain a large proportion of the differences
298 in the effect of substitutions on different backgrounds.

299

300 **A global analysis of ATP1A sequences reveals further constraints on the evolution of CTS** 301 **resistance**

302

303 Since our functional experiments were necessarily limited in scope, we carried out a broad
304 phylogenetic analysis to evaluate how well our findings align with global estimates of rates of
305 convergence for the ATP1A family beyond ATP1A1 and beyond sites implicated in CTS resistance.
306 Using a multisequence alignment of 831 ATP1A protein sequences, including the three ATP1A
307 paralogs shared among tetrapods (i.e., amphibians, non-avian reptiles, birds, and mammals), we
308 inferred a maximum likelihood phylogeny of the gene family (Fig. S1). We then used ancestral
309 sequence reconstruction to infer the history of substitution events on all branches in the tree and
310 counted the number of convergent amino acid substitutions per site along the entire protein (see
311 Materials and Methods). Convergent substitutions are defined as substitutions on two branches at
312 the same site resulting in the same amino acid state. Interestingly, we did not detect a correlation
313 between the relative number of convergent substitutions with overall ATP1A divergence across the

314 tree (Fig. S5). This result also held true when considering only substitutions to the key CTS-
315 resistance sites 111 and 122 (Fig. S7).

316

317 To gain further insights into the factors that determine convergent evolution in ATP1A, we looked
318 more closely at patterns of individual convergent substitutions at sites 111 and 122 by extracting
319 each convergent substitution and visualizing its distribution along the sequence divergence axis
320 (Fig. 6A). Under the expectation that rates of convergence should tend to decrease as a function
321 of sequence divergence due to prevalent epistasis, the distribution of pairwise convergent events
322 along the sequence divergence axis should be left-skewed, with a peak towards lower sequence
323 divergence. In contrast to this expectation, the distribution is bimodal, with one peak at 0.33 and
324 the other at 0.69 substitutions/site (Fig. 6B bottom panel). Convergent substitutions have occurred
325 almost across the full range of protein divergence estimates. For example, if X is any starting state,
326 the substitution X111R has occurred independently in 13 tetrapod lineages and X111L
327 independently in 20 lineages. Both substitutions have a broad phylogenetic distribution, suggesting
328 that their effects do not strongly depend on sequence states at a large number of sites throughout
329 the protein. Interestingly, however, the distributions for X111H and X111E substitutions are
330 relatively left-skewed, in line with epistasis for CTS resistance that we observed in experiments for
331 H111E/E111H (Fig 4E).

332

333 Using this same 831-sequence, 3-paralog alignment, we also asked which sites across all paralogs
334 have substitution patterns that are most strongly correlated with those at 111 and 122 (Methods).
335 We found 4 sites (102, 112, 527 and 676) that stand out as being in the top 5% of sites most
336 strongly correlated with substitutions at both 111 and 122 (Fig. 6B), and this amount of overlap was
337 larger than expected by chance. Further, the top 5% of sites most strongly correlated with site 111
338 also tend to be closer to 111 in atomic distance than expected (median distance to 111: 25.1 Å, p
339 $< 5e-4$, bootstrap; Fig. 6C). Combining the results from our phylogenetic and functional analyses
340 we identified a set of substitutions that are both strongly correlated with changes in 111 and 122
341 and account for a substantial proportion of the variance in background-dependent effects in our
342 functional experiments (overlaps are larger than expected by chance; Fig 6B). For instance, despite
343 being independently ascertained, site 102 is also among the most strongly predictive sites for
344 background-dependent effects in our functional experiments, belonging to a group of 6 sites that
345 explains 60% of variance (Fig. 5B and Fig. 6B). Together, our results suggest that proximate
346 interactions involving a small number of sites, particularly site 111, are likely to be an important
347 determinant of background-dependent effects.

348

349 **Discussion**

350

351 Previous work has shown that the adaptive evolution of NKA-mediated CTS resistance in animals
352 is constrained by pleiotropy and epistasis (i.e., background-dependence) [5,23–25,30]. Further,
353 based on broad phylogenetic analysis of proteomes, our *a priori* expectation is that epistasis should
354 represent a stronger constraint with increasing levels of divergence between species and ATP1A
355 paralogs [20]. In light of these considerations, our extensive survey of the ATP1A gene family in
356 tetrapods reveals two striking and seemingly contradictory patterns. The first is that some
357 substitutions underlying CTS resistance in tetrapods are broadly distributed phylogenetically and
358 even shared with insects (e.g., N122H is widespread among snakes and found in the monarch
359 butterfly and other insects; see Fig. 3 for more examples). Patterns like these suggest that epistatic
360 constraints have a limited role in the evolution of CTS resistance, as the same mutation can be
361 favored on highly divergent genetic backgrounds. On the other hand, there is also substantial
362 diversity in resistance-conferring states at sites 111 and 122, and some combinations of these
363 substitutions appear to be phylogenetically restricted. For example, the CTS-resistant combination
364 of Q111R+N122D has evolved multiple times in tetrapods but is absent in insects, whereas the
365 CTS-resistant combination Q111V+N122H evolved multiple times in insects but is absent in
366 tetrapods (Fig 3). Additionally, some substitutions also appear to be paralog-specific in tetrapods
367 (Fig 3). These phylogenetic signatures suggest at least some role for epistasis as a source of
368 contingency in the evolution of ATP1A-mediated CTS resistance in animals, i.e., that the fitness
369 effects of substitutions depend on the order in which they occur. How can these disparate patterns
370 be reconciled? To what extent do genetic background and contingency limit the evolution of CTS
371 resistance in animals?

372

373 In our functional analysis of diverse ATP1A1 proteins, we find that derived substitutions at sites
374 111 and 122 have largely predictable effects on CTS resistance, with salient exceptions that tend
375 to be in size rather than direction (Fig. 4). For example, Q111R contributes to CTS resistance on
376 many species' backgrounds, but not on that of sandgrouse (Fig. 4C and 4E). We also note that
377 species with identical paired states at 111 and 122 can vary in CTS resistance by more than an
378 order of magnitude (Fig. 4B). Together, these patterns point to background determinants of CTS
379 resistance that may be additive rather than epistatic. Despite this, there are some substitutions that
380 are widely distributed phylogenetically, such as N122D, that nonetheless do exhibit background-
381 dependent effects on CTS resistance (Fig. 4C and 4E).

382

383 With respect to pleiotropic effects on NKA activity, our functional analysis of substitutions at sites
384 111 and 122 on diverse ATP1A1 backgrounds suggest that interactions between these
385 substitutions and those backgrounds are largely additive. Specifically, we find that the severity of

386 the effect of a particular CTS resistance substitution on NKA activity does not differ if added to
387 protein backgrounds that are in the range of 49 to 86 amino acid substitutions away from the protein
388 background on which that substitution naturally occurs (Fig. 5). In light of previous results
389 demonstrating background-dependent effects of similar substitutions on NKA activity [23–25], our
390 findings suggest that the extent of epistasis does not have a monotonic dependence on the extent
391 of ATP1A1 divergence. Our findings further support increasing evidence that while epistasis is likely
392 to be a pervasive feature of protein evolution, many mutational effects on structural and functional
393 properties of proteins nonetheless seem to be additive (e.g., [37–39]).

394

395 We propose that our observations can be reconciled with previous results demonstrating epistatic
396 constraints if epistasis with respect to protein function is confined to a small number of sites in the
397 protein. If so, we might expect that the magnitude of epistasis may have little dependence on the
398 extent of protein-wide ATP1A1 divergence but would instead be better predicted by divergence at
399 a few key sites. In support of this view, Mohammadi et al. [25] showed that decreases in ATP1A1
400 enzyme activity due to substitutions Q111R and N122D can be rescued by 10 (or fewer) of the 19
401 amino acid differences distinguishing the backgrounds of CTS-resistant and sensitive ATP1A1
402 paralogs of grass frogs. Further, studies in *Drosophila melanogaster* [23,24] show that severe
403 neural dysfunction associated with CTS resistance substitutions at sites 111 and 122 can largely
404 be rescued with one additional substitution (A119S). Our study lends further support to this view
405 by showing that one can identify a small group of sites (16 or fewer) that account for a large
406 proportion of the variation in background-dependent effects on enzyme activity across proteins
407 spanning the breadth of the tetrapod phylogeny.

408

409 Phenotypes such as enzyme activity are not equivalent to organismal fitness and that there may
410 be a nonlinear mapping between the two. The discussion above assumes that changes in enzyme
411 activity are most likely detrimental to organismal fitness, but this need not be the case. We found
412 that the activity of wild-type NKAs varies 6-fold among the species surveyed (Fig. 4E), suggesting
413 that most species are either robust to changes in NKA activity or that changes have occurred in
414 other genes (including other ATP1A paralogs) to compensate for changes in NKA activity
415 associated with ATP1A1. Thus, either protein activity itself is not an important pleiotropic constraint
416 on the evolution of CTS resistance of NKA, or constraint depends not just on the protein background
417 but also on the broader genetic background of the organism (e.g., other interacting proteins; see
418 [23]).

419

420 Our work highlights the utility of comparative functional work in understanding the nature of epistatic
421 constraints on the evolution of novel protein functions. In this case-study of the evolution of CTS-

422 resistant NKAs, we find that epistatic constraints are more likely to depend on divergence at a small
423 number of key sites in the protein, likely in close proximity to site 111, rather than overall levels of
424 protein divergence. The circumscribed nature of these constraints may account for the remarkable
425 convergence of CTS-resistance substitutions observed among the NKAs of highly divergent
426 species.

427

428

429

430 **Materials and Methods**

431

432 **Sample collection and data sources.**

433 In order to carry out a comprehensive survey of vertebrate ATP1A paralogs (ATP1A1, ATP1A2 and
434 ATP1A3), we collated a total of 831 protein sequences for this study (corresponding alignment can
435 be found in Supplementary Dataset 1). Mammals possess a fourth paralog (ATP1A4) that is
436 expressed predominantly in testes [40] that we did not consider here, although for completeness
437 the protein sequences are provided in Supplementary Dataset 1 and the alignment of variant sites
438 in Supplementary Dataset 2). The 831 sequences included RNA-seq data generated here for 27
439 species of non-avian reptiles (Table S1; PRJNA754197) to provide more information from some
440 previously underrepresented lineages. These included field-caught and museum-archived
441 specimens as well as animals purchased from commercial pet vendors. Purchased animals were
442 processed following the procedures specified in the IACUC Protocol No. 2057-16 (Princeton
443 University) and implemented by a research veterinarian at Princeton University. Wild-caught
444 animals were collected under Colombian umbrella permit *resolución No. 1177* granted by the
445 *Autoridad Nacional de Licencias Ambientales* to the Universidad de los Andes and handled
446 according to protocols approved by the Institutional Committee on the Care and Use of Laboratory
447 Animals (abbreviated *CICUAL* in Spanish) of the Universidad de los Andes. In all cases, fresh
448 tissues (brain, stomach, and muscle) were taken and preserved in RNeasy (Invitrogen) and stored
449 at -80°C until used.

450

451 **Reconstruction of ATP1A paralogs.**

452 RNA-seq libraries were prepared either using TruSeq RNA Library Prep Kit v2 (Illumina) and
453 sequenced on Illumina HiSeq2500 (Genomics Core Facility, Princeton, NJ, USA) or using NEBNext
454 Ultra RNA Library Preparation Lit (NEB) and sequenced on Illumina HiSeq4000 (Genewiz, South
455 Plainfield, NJ, USA) (Table S2). All raw RNA-seq data generated for this study have been deposited
456 in the National Center for Biotechnology Information (NCBI) Sequence Read Archive (SRA) under
457 Bioproject PRJNA754197. Together with SRA datasets downloaded from public database, reads
458 were trimmed to Phred quality ≥ 20 and length ≥ 20 and then assembled *de novo* using Trinity
459 v2.2.0 [41]. Sequences of ATP1A paralogs 1, 2 and 3 were pulled out with BLAST searches (blast-
460 v2.26), individually curated, and then aligned using ClustalW. Complete alignments of ATP1/2/3
461 can be found in Supplementary Dataset 1.

462

463 **Statistical phylogenetic analyses**

464 We use the standard sheep (*Ovis aries*) numbering system to match previous literature; this
465 number corresponds to the Uniprot:P04074 sequence minus 5 residues from the 5' end. Protein
466 sequences from ATP1A1 (N=429), ATP1A2 (N=197) and ATP1A3 (N=205) including main tetrapod

467 classes (amphibians, non-avian reptiles, birds, and mammals) plus lungfish and coelacanth as
468 outgroups were aligned using ClustalW with default parameters. The optimal parameters for
469 phylogenetic reconstruction were taken from the best-fit amino acid substitution model based on
470 Akaike Information Criterion (AIC) as implemented in ModelTest-NG v.0.1.5 [42], and was inferred
471 to be JTT+G4+F. An initial phylogeny was inferred using RAxML HPC v.8 [43] under the
472 JTT+GAMMA model with empirical amino acid frequencies. Branch lengths and node support
473 (aLRS) were further refined using PhyML v.3.1 [44] with empirical amino acid frequencies and
474 maximum likelihood estimates of rate heterogeneity parameters, I and Γ . Phylogeny visualization
475 and mapping of character states for each paralog was done using the R package ggtree [45].

476

477 **Ancestral sequence reconstruction and convergence calculations**

478 Ancestral sequence reconstruction was performed in PAML using codeml [46] under the JTT+G4+F
479 substitution model. Ancestral sequences from all nodes in the ATP1A phylogeny were combined
480 with extant sequences to produce a 1040 amino-acid multiple sequence alignment of 1,660 ATP1A
481 proteins (831 extant species and 829 inferred ancestral sequences; Fig. S1). For each branch in
482 the tree, we determined the occurrence of substitutions by using the ancestral and derived amino
483 acid states at each site using only states with posterior probability (PP) > 0.8. All branch pairs were
484 compared, except sister branches and ancestor-descendent pairs [20,21]. When comparing
485 substitutions on two distinct branches at the same site, substitutions to the same amino acid state
486 were counted as convergences, while substitutions away from a common amino acid were counted
487 as divergences. We excluded a putative 30 amino acid-long alternatively-spliced region (positions
488 810-840). For each pairwise comparison, we calculated the proportion of observed convergent
489 events per branch as (number of convergences +1) / (number of divergences +1). The line
490 describing the trend was calculated as a running average with a window size of 0.05
491 substitutions/site. 95% confidence intervals were estimated based on 100 random samples of
492 pairwise branch comparisons for each window. To determine whether convergence at sites 111
493 or 122 decreases with sequence divergence, we encoded convergence events as “1” and
494 divergence events as “0” for all pairwise sequence comparisons and used a logistic regression to
495 test for the correlation between molecular convergence (0 or 1) and genetic distance (Fig. S4).

496 **Identifying correlated substitutions.**

497 We used BayesTraits [47] to detect sites across the ATP1A phylogeny that exhibit correlated
498 evolution with sites 111 and 122. Using the reconstructed ancestral sequences for each paralogous
499 clade (i.e., the most recent common ancestor (MRCA) of ATP1A1, the MRCA of ATP1A2, and the
500 MRCA of ATP1A3), we coded each amino acid state among extant sequences of the multi-species
501 alignment into ancestral ‘0’ and derived ‘1’ states, and used these plus the phylogeny with

502 estimated branch lengths as inputs for BayesTraits. BayesTraits fits a continuous-time Markov
503 model to estimate transition rates between discrete, binary traits and estimates the best fitting
504 model describing their joint evolution on a phylogeny. Specifically, we tested whether the rate of
505 evolution at sites 111 and 122 was dependent on all other variant sites (see below). We excluded
506 singleton sites and sites with more than 80% gaps, as these sites would be of little information,
507 resulting in an analysis of 417 variant sites.

508 We tested two sets of models, hereafter referred as base and restricted models, each of which has
509 a null independent and an alternative dependent model. The null independent model assumes that
510 the two sites evolve independently, and the alternative dependent model assumes that the sites
511 are correlated such that the change at one site is dependent on the state at the other site. Because
512 the null model is a general form of the alternative model, both models can be compared under a
513 likelihood ratio test (LRT) with degrees of freedom (df) equal to the difference in the number of
514 parameters between models. The base and restricted sets of models differ on the presence of
515 restricted parameters for certain transition rates, and consequently differ in the number of df. In the
516 base models, the null model has four rate parameters describing each possible independent
517 change of state at each site; the alternative model has eight rate parameters describing all possible
518 changes at each site dependent on the state at the other site (LRT with $df=4$). For the restricted
519 models, we set the rates of transition to the ancestral state to zero [23] as the median branch length
520 of the tree of 0.002351 substitutions per site makes it unlikely for a site to change twice or back to
521 the ancestral state. After these restrictions, the null independent model had four transition
522 parameters. To test for dependence, we imposed two additional restrictions to the model: one
523 forcing the transition rate at site one to be fixed regardless of the state of site 2 ($q_{13}=q_{24}$), and a
524 second forcing the transition rate at site 2 to be fixed regardless of the state of site 1 ($q_{12}=q_{34}$)
525 [23]. This effectively tests whether the transition rate is affected by the state of either site and leaves
526 the model with only two transition parameters (LRT with $df=2$). To run the analysis, the phylogeny
527 branch lengths were scaled using BayesTraits to have a mean length of 0.1, and to increase the
528 chance of finding the true maximum likelihood, we set MLTries to 250.

529 **Protein structure analysis.**

530 To test for spatial clustering of sites showing statistical signatures of coevolution with site 111 or
531 122, we used a custom Python script (available on request) and the Bio.PDB's module. We used
532 the crystal structure of Na,K-ATPase (PDB: 3b8e) to estimate distances (in Angstroms) between
533 the alpha carbon of site 111 or 122 to the alpha carbon of all other variable sites in the alignment.
534 We calculated the median distance of the top 5% of variable sites with the strongest signature of
535 correlated evolution with each focal site, 111 or 122 (from BayesTraits output). We estimated the

536 p-value using 1000 random samples of 5% of variable sites and calculating the proportion of times
537 the median value was less than or equal to the observed value.

538

539 **Construction of expression vectors.**

540 ATP1A1 and ATP1B1 wild-type sequences for the eight selected tetrapod species (Fig. 4) were
541 synthesized by Invitrogen™ GeneArt. The β 1-subunit genes were inserted into pFastBac Dual
542 expression vectors (Life Technologies) at the p10 promoter with XhoI and PaeI (FastDigest Thermo
543 Scientific™) and then control sequenced. The α 1-subunit genes were inserted at the PH promoter
544 of vectors already containing the corresponding β 1-subunit proteins using In-Fusion® HD Cloning
545 Kit (Takara Bio, USA Inc.) and control sequenced. All resulting vectors had the α 1-subunit gene
546 under the control of the PH promoter and a β 1-subunit gene under the p10 promoter. The resulting
547 eight vectors were then subjected to site-directed mutagenesis (QuickChange II XL Kit; Agilent
548 Technologies, La Jolla, CA, USA) to introduce the codons of interest. In total, 21 vectors were
549 produced (Table S3).

550

551 **Generation of recombinant viruses and transfection into Sf9 cells.**

552 *Escherichia coli* DH10bac cells harboring the baculovirus genome (bacmid) and a transposition
553 helper vector (Life Technologies) were transformed according to the manufacturer's protocol with
554 expression vectors containing the different gene constructs. Recombinant bacmids were selected
555 through PCR screening, grown, and isolated. Subsequently, Sf9 cells (4×10^5 cells*ml) in 2 ml of
556 Insect-Xpress medium (Lonza, Walkersville, MD, USA) were transfected with recombinant bacmids
557 using Cellfectin reagent (Life Technologies). After a three-day incubation period, recombinant
558 baculoviruses were isolated (P1) and used to infect fresh Sf9 cells (1.2×10^6 cells*ml) in 10 ml of
559 Insect-Xpress medium (Lonza, Walkersville, MD, USA) with 15 mg/ml gentamycin (Roth, Karlsruhe,
560 Germany) at a multiplicity of infection of 0.1. Five days after infection, the amplified viruses were
561 harvested (P2 stock).

562

563 **Preparation of Sf9 membranes.**

564 For production of recombinant NKA, Sf9 cells were infected with the P2 viral stock at a multiplicity
565 of infection of 10^3 . The cells (1.6×10^6 cells*ml) were grown in 50 ml of Insect-Xpress medium
566 (Lonza, Walkersville, MD, USA) with 15 mg/ml gentamycin (Roth, Karlsruhe, Germany) at 27°C in
567 500 ml flasks (35). After 3 days, Sf9 cells were harvested by centrifugation at 20,000 x g for 10 min.
568 The cells were stored at -80 °C and then resuspended at 0 °C in 15 ml of homogenization buffer
569 (0.25 M sucrose, 2 mM EDTA, and 25 mM HEPES/Tris; pH 7.0). The resuspended cells were
570 sonicated at 60 W (Bandelin Electronic Company, Berlin, Germany) for three 45 s intervals at 0 °C.
571 The cell suspension was then subjected to centrifugation for 30 min at 10,000 x g (J2-21 centrifuge,

572 Beckmann-Coulter, Krefeld, Germany). The supernatant was collected and further centrifuged for
573 60 m at 100,000 x g at 4 °C (Ultra- Centrifuge L-80, Beckmann-Coulter) to pellet the cell
574 membranes. The pelleted membranes were washed once and resuspended in ROTIPURAN® p.a.,
575 ACS water (Roth) and stored at -20 °C. Protein concentrations were determined by Bradford assays
576 using bovine serum albumin as a standard. Three biological replicates were produced for each
577 NKA construct.

578

579 **Verification by SDS-PAGE/western blotting.**

580 For each biological replicate, 10 µg of protein were solubilized in 4x SDS-polyacrylamide gel
581 electrophoresis sample buffer and separated on SDS gels containing 10% acrylamide.
582 Subsequently, they were blotted on nitrocellulose membrane (HP42.1, Roth). To block non-specific
583 binding sites after blotting, the membrane was incubated with 5% dried milk in TBS-Tween 20 for
584 1 h. After blocking, the membranes were incubated overnight at 4 °C with the primary monoclonal
585 antibody α5 (Developmental Studies Hybridoma Bank, University of Iowa, Iowa City, IA, USA).
586 Since only membrane proteins were isolated from transfected cells, detection of the α subunit also
587 indicates the presence of the β subunit. The primary antibody was detected using a goat-anti-
588 mouse secondary antibody conjugated with horseradish peroxidase (Dianova, Hamburg,
589 Germany). The staining of the precipitated polypeptide-antibody complexes was performed by
590 addition of 60 mg 4-chloro-1 naphthol (Sigma-Aldrich, Taufkirchen, Germany) in 20 ml ice-cold
591 methanol to 100 ml phosphate buffered saline (PBS) containing 60 µl 30% H₂O₂. See Fig. S8.

592

593 **Ouabain inhibition assay.**

594 To determine the sensitivity of each NKA construct against cardiotonic steroids (CTS), we used the
595 water-soluble cardiac glycoside, ouabain (Acrōs Organics), as our representative CTS. 100 µg of
596 each protein was pipetted into each well in a nine-well row on a 96-well microplate (Fisherbrand)
597 containing stabilizing buffers (see buffer formulas in [48]). Each well in the nine-well row was
598 exposed to exponentially decreasing concentrations of ouabain (10⁻³ M, 10⁻⁴ M, 10⁻⁵ M, 10⁻⁶ M, 10⁻⁷
599 M, 10⁻⁸ M, dissolved in distilled H₂O), plus distilled water only (experimental control), and a
600 combination of an inhibition buffer lacking KCl and 10⁻² M ouabain to measure background protein
601 activity [48]. The proteins were incubated at 37°C and 200 rpms for 10 minutes on a microplate
602 shaker (Quantifoil Instruments, Jena, Germany). Next, ATP (Sigma Aldrich) was added to each
603 well and the proteins were incubated again at 37°C and 200 rpms for 20 minutes. The activity of
604 NKA following ouabain exposure was determined by quantification of inorganic phosphate (Pi)
605 released from enzymatically hydrolyzed ATP. Reaction Pi levels were measured according to the
606 procedure described in Taussky and Shorr [49] (see Petschenka et al. [48]). All assays were run in
607 duplicate and the average of the two technical replicates was used for subsequent statistical

608 analyses. Absorbance for each well was measured at 650 nm with a plate absorbance reader
609 (BioRad Model 680 spectrophotometer and software package). See Table S4.

610

611 **ATP hydrolysis assay.**

612 To determine the functional efficiency of different NKA constructs, we calculated the amount of Pi
613 hydrolyzed from ATP per mg of protein per minute. The measurements (the mean of two technical
614 replicates) were obtained from the same assay as described above. In brief, absorbance from the
615 experimental control reactions, in which 100 μ g of protein was incubated without any inhibiting
616 factors (i.e., ouabain or buffer excluding KCl), were measured and translated to mM Pi from a
617 standard curve that was run in parallel (1.2 mM Pi, 1 mM Pi, 0.8 mM Pi, 0.6 mM Pi, 0.4 mM Pi, 0.2
618 mM Pi, 0 mM Pi). See Table S4.

619

620 **Statistical analyses of functional data.**

621 ATPase activity in the presence and absence of the CTS ouabain was measured following
622 Petschenka et al. [48]. Background phosphate absorbance levels from reactions with inhibiting
623 factors were used to calibrate phosphate absorbance. For ouabain sensitivity measurements, these
624 calibrated absorbance values were converted to percentage non-inhibited NKA activity based on
625 measurements from the control wells (as above). For each of the 3 biological replicates, log₁₀ IC₅₀
626 values were estimated using a four-parameter logistic curve, with the top asymptote set to 100 and
627 the bottom asymptote set to zero, using the nlsLM function of the minipack.lm library in R [25]. To
628 measure baseline recombinant protein activity, the calculated Pi concentrations of 100 μ g of protein
629 assayed in the absence of ouabain were converted to nmol Pi/mg protein/min. We used paired *t*-
630 tests with Bonferroni corrections to identify significant differences between constructs with and
631 without engineered substitutions. We used a two-way ANOVA to test for background dependence
632 of substitutions (i.e., interaction between background and amino acid substitution) with respect to
633 ouabain resistance (log₁₀ IC₅₀) and protein activity. Specifically, we tested whether the effects of a
634 substitution X->Y are equal on different backgrounds (null hypothesis: X->Y (background 1) = X-
635 >Y (background 2)). We further assumed that the effects of a substitution X->Y should match that
636 of Y->X. All statistical analyses were implemented in R. Data were plotted using the ggplot2
637 package in R.

638

639 Additionally, we evaluated the relationship between the effect of substitutions to a given amino acid
640 state and the extent of sequence divergence between the protein backgrounds on which these
641 substitutions were tested. To do this, we first calculated the effect of introducing a derived amino
642 acid state as the percent change in protein activity relative to the wild-type protein. For example,
643 the effect of the mutation N122D in Chinchilla (CHI) is

644
$$E_{CHI,N122D} = [(CHI_{N122D}) - (CHI_{wt})] / (CHI_{wt}) \times 100;$$

645 We then calculated the absolute difference between effects of substitutions to the same amino acid
646 on two different backgrounds. For example, the difference (Δ) in the effect of 122D when introduced
647 to the Chinchilla (CHI, mammal) and false fer-de-lance (FER, snake) proteins is

648
$$\Delta_{CHI-FER,X122D} = |E_{CHI,N122D} - E_{FER,H122D}|.$$

649 These calculations were possible for 11 pairwise comparisons (4 for site 111 and 7 for site 122;
650 Table S7). We then evaluated the relationship between the estimated differences in the effects of
651 substitutions to a given state versus the extent of protein sequence divergence (number of amino
652 acid differences) between wild-type backgrounds.

653

654 To identify variant sites that most strongly predicted background-dependent effects in our data, we
655 employed a site-by-site ANOVA analysis. For each of the eleven pairwise comparisons (e.g.,
656 $\Delta_{CHI-FER,X122D}$) each variant site was encoded as '0' or '1' if the wild-type sequences had the same
657 or different amino acid state, respectively. This binarized per-site divergence (0 or 1) was used as
658 the dependent variable in the ANOVA, with sites 111 or 122 (the mutated sites) as a covariate (Fig.
659 S5A). For each of the 113 variant sites among the eight wild-type proteins, we then estimated that
660 site's marginal variance explained.

661

662 Given the limited number of wild-type backgrounds (8) relative to the number of sites (113), and
663 use of constructs in multiple comparisons, strong correlations occur some variant sites (Fig. S5B).
664 We thus grouped sites according to how they partition the divergence in experimental pairwise
665 sequence comparisons. Grouping sites with Pearson's $r > 0.8$ results in 24 groups. Using one
666 representative site per group, we then fitted nested ANOVA models to determine how much of
667 variation in the Δ is explained by adding an additional group of sites, adding groups in the order of
668 largest (group 1) to smallest (group 24) amount of variance explained. Using Likelihood Ratio Tests
669 (LRTs) and Akaike's Information Criteria (AIC), we identified the best model as the one including
670 only the first two groups, which represent a total of 16 sites (14 sites in group 1 and two sites in
671 group 2; Fig. S5C and Table S9). These 16 sites account for 78% of the variance (ANOVA R^2).
672 Since groups 1 and 2 were ascertained as those accounting for the largest proportion of the
673 variance, we established the significance of this observation by permutation. Specifically, we
674 performed 10,000 permutations of the experimental pairwise Δ across construct comparisons and
675 repeated the procedure that was applied to the observed data to obtain a null distribution of R^2
676 values. The p-value is estimated as the probability of finding two groups of sites that explain $R^2 \geq$
677 0.78. We further evaluated the extent of correlation (estimated as Pearson's r) between Δ and

678 sequence divergence at the 16 sites identified above. Similarly, to test for the significance of our
679 regression model between Δ and divergence, we estimated the p-value as the probability of
680 observing a Pearson's r of 0.78 (or R^2 of 0.61) or larger based on 10,000 permuted samples
681 (permuting effects, Δ , across construct comparisons). To determine the robustness of our results
682 to the grouping criteria, we did the same analyses using a higher cutoff of Pearson's $r > 0.99$ (Table
683 S8).

684

685

686 **Acknowledgments**

687

688 We thank G. Sella and M. Przeworski for helpful discussions, and M. Przeworski for critical reading
689 of an early draft of this paper. We thank C. Natarajan, P. Kowalski, M. Winter, and V. Wagschal for
690 assistance in the laboratory, and D.A. Gómez-Sánchez for assistance in the field. We thank J. Oaks
691 for providing tissue from ring-necked snake. We thank the Vice-president's Office for Research and
692 Creation of the Universidad de los Andes for help with permits. This study was funded by grants
693 from the National Institutes of Health to PA (R01-GM115523), JFS (R01-HL087216) and SM (F32-
694 HL149172), the National Science Foundation (OIA-1736249) to JFS, the Deutsche
695 Forschungsgemeinschaft (Do 517/10-1) to SD, and the Alexander von Humboldt Foundation to
696 SM.

697

698 **References**

- 699
- 700 1. Stern DL. The genetic causes of convergent evolution. *Nat Rev Genet.* 2013;14: 751–764.
- 701 2. Storz JF. Causes of molecular convergence and parallelism in protein evolution. *Nat Rev*
702 *Genet.* 2016;17: 239.
- 703 3. Lingrel JB. The physiological significance of the cardiotonic steroid/ouabain-binding site of
704 the Na, K-ATPase. *Annu Rev Physiol.* 2010;72: 395–412.
- 705 4. Dobler S, Dalla S, Wagschal V, Agrawal AA. Community-wide convergent evolution in insect
706 adaptation to toxic cardenolides by substitutions in the Na, K-ATPase. *Proc Natl Acad Sci.*
707 2012;109: 13040–13045.
- 708 5. Zhen Y, Aardema ML, Medina EM, Schumer M, Andolfatto P. Parallel molecular evolution
709 in an herbivore community. *science.* 2012;337: 1634–1637.
- 710 6. Moore DJ, Halliday DC, Rowell DM, Robinson AJ, Keogh JS. Positive Darwinian selection
711 results in resistance to cardioactive toxins in true toads (*Anura: Bufonidae*). *Biol Lett.*
712 2009;5: 513–516.
- 713 7. Ujvari B, Casewell NR, Sunagar K, Arbuckle K, Wüster W, Lo N, et al. Widespread
714 convergence in toxin resistance by predictable molecular evolution. *Proc Natl Acad Sci.*
715 2015;112: 11911–11916.
- 716 8. Mohammadi S, Gompert Z, Gonzalez J, Takeuchi H, Mori A, Savitzky AH. Toxin-resistant
717 isoforms of Na⁺/K⁺-ATPase in snakes do not closely track dietary specialization on toads.
718 *Proc R Soc B Biol Sci.* 2016;283: 20162111.
- 719 9. Mohammadi S, Yang L, Matthew B, Rowland HM. Defence mitigation by predators of
720 chemically defended prey integrated over the predation cycle and across biological levels.
721 *EcoEvoRxiv.* 2022. doi:doi:10.32942/osf.io/74xu2
- 722 10. Groen S, Whiteman N. Convergent evolution of cardiac-glycoside resistance in predators
723 and parasites of milkweed herbivores. *Curr Biol.* 2021;31: R1465–R1466.
724 doi:10.1016/j.cub.2021.10.025
- 725 11. Stern DL. *Evolution, development, & the predictable genome.* Roberts and Co. Publishers;
726 2011.
- 727 12. Phillips PC. Epistasis—the essential role of gene interactions in the structure and evolution
728 of genetic systems. *Nat Rev Genet.* 2008;9: 855–867.
- 729 13. Fitch W. Rate of change of concomitantly variable codons. *J Mol Evol.* 1971;1: 84–96.
- 730 14. Callahan B, Neher RA, Bachtrog D, Andolfatto P, Shraiman BI. Correlated evolution of
731 nearby residues in *Drosophilid* proteins. *PLoS Genet.* 2011;7: e1001315.

- 732 15. Starr TN, Thornton JW. Epistasis in protein evolution. *Protein Sci.* 2016;25: 1204–1218.
- 733 16. Storz JF. Compensatory mutations and epistasis for protein function. *Curr Opin Struct Biol.*
734 2018;50: 18–25.
- 735 17. Pollock DD, Thiltgen G, Goldstein RA. Amino acid coevolution induces an evolutionary
736 Stokes shift. *Proc Natl Acad Sci.* 2012;109: E1352. doi:10.1073/pnas.1120084109
- 737 18. Shah P, McCandlish DM, Plotkin JB. Contingency and entrenchment in protein evolution
738 under purifying selection. *Proc Natl Acad Sci.* 2015;112: E3226.
739 doi:10.1073/pnas.1412933112
- 740 19. Pokusaeva VO, Usmanova DR, Putintseva EV, Espinar L, Sarkisyan KS, Mishin AS, et al. An
741 experimental assay of the interactions of amino acids from orthologous sequences shaping
742 a complex fitness landscape. *PLoS Genet.* 2019;15: e1008079.
- 743 20. Goldstein RA, Pollard ST, Shah SD, Pollock DD. Nonadaptive amino acid convergence rates
744 decrease over time. *Mol Biol Evol.* 2015;32: 1373–1381.
- 745 21. Zou Z, Zhang J. Are convergent and parallel amino acid substitutions in protein evolution
746 more prevalent than neutral expectations? *Mol Biol Evol.* 2015;32: 2085–2096.
- 747 22. Zou Z, Zhang J. Gene tree discordance does not explain away the temporal decline of
748 convergence in mammalian protein sequence evolution. *Mol Biol Evol.* 2017;34: 1682–
749 1688.
- 750 23. Taverner AM, Yang L, Barile ZJ, Lin B, Peng J, Pinharanda AP, et al. Adaptive substitutions
751 underlying cardiac glycoside insensitivity in insects exhibit epistasis in vivo. O’Connell LA,
752 Wittkopp PJ, O’Connell LA, Zakon HH, Courtier-Orgogozo V, editors. *eLife.* 2019;8: e48224.
753 doi:10.7554/eLife.48224
- 754 24. Karageorgi M, Groen SC, Sumbul F, Pelaez JN, Verster KI, Aguilar JM, et al. Genome editing
755 retraces the evolution of toxin resistance in the monarch butterfly. *Nature.* 2019;574: 409–
756 412. doi:10.1038/s41586-019-1610-8
- 757 25. Mohammadi S, Yang L, Harpak A, Herrera- Álvarez S, Rodríguez-Ordoñez M del P, Peng J, et
758 al. Concerted evolution reveals co-adapted amino acid substitutions in frogs that prey on
759 toxic toads. *Curr Biol.* 2021;31: 2530-2538.e10. doi:10.1016/j.cub.2021.03.089
- 760 26. Sweadner KJ, Arystarkhova E, Penniston JT, Swoboda KJ, Brashear A, Ozelius LJ. Genotype-
761 structure-phenotype relationships diverge in paralogs ATP1A1, ATP1A2, and ATP1A3.
762 *Neurol Genet.* 2019;5: e303–e303. doi:10.1212/NXG.0000000000000303
- 763 27. Ujvari B, Mun H, Conigrave AD, Bray A, Osterkamp J, Halling P, et al. Isolation breeds
764 naivety: island living robs Australian varanid lizards of toad-toxin immunity via four-base-
765 pair mutation. *Evol Int J Org Evol.* 2013;67: 289–294.

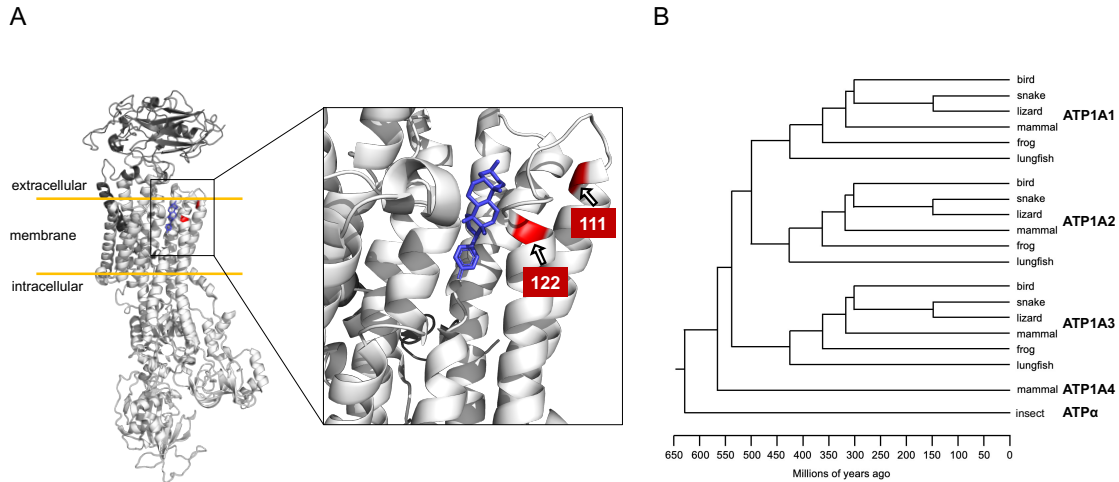
- 766 28. Marshall BM, Casewell NR, Vences M, Glaw F, Andreone F, Rakotoarison A, et al.
767 Widespread vulnerability of Malagasy predators to the toxins of an introduced toad. *Curr*
768 *Biol.* 2018;28: R654–R655.
- 769 29. Lunzer M, Golding GB, Dean AM. Pervasive cryptic epistasis in molecular evolution. *PLoS*
770 *Genet.* 2010;6: e1001162.
- 771 30. Yang L, Ravikanthachari N, Mariño-Pérez R, Deshmukh R, Wu M, Rosenstein A, et al.
772 Predictability in the evolution of Orthopteran cardenolide insensitivity. *Philos Trans R Soc*
773 *B.* 2019;374: 20180246.
- 774 31. Price EM, Lingrel JB. Structure-function relationships in the sodium-potassium ATPase.
775 alpha. subunit: site-directed mutagenesis of glutamine-111 to arginine and asparagine-122
776 to aspartic acid generates a ouabain-resistant enzyme. *Biochemistry.* 1988;27: 8400–8408.
- 777 32. Stoltzfus A, McCandlish DM. Mutational Biases Influence Parallel Adaptation. *Mol Biol Evol.*
778 2017;34: 2163–2172. doi:10.1093/molbev/msx180
- 779 33. Zhang J, Kumar S. Detection of convergent and parallel evolution at the amino acid
780 sequence level. *Mol Biol Evol.* 1997;14: 527–536.
- 781 34. Toledo LF, Ribeiro R, Haddad CF. Anurans as prey: an exploratory analysis and size
782 relationships between predators and their prey. *J Zool.* 2007;271: 170–177.
- 783 35. Dobler S, Wagschal V, Pietsch N, Dahdouli N, Meinzer F, Romey-Glusing R, et al. New ways
784 to acquire resistance: imperfect convergence in insect adaptations to a potent plant toxin.
785 *Proc R Soc B.* 2019;286: 20190883.
- 786 36. Clausen MV, Hilbers F, Poulsen H. The structure and function of the Na, K-ATPase isoforms
787 in health and disease. *Front Physiol.* 2017;8: 371.
- 788 37. Wells JA. Additivity of mutational effects in proteins. *Biochemistry.* 1990;29: 8509–8517.
- 789 38. Lunzer M, Miller SP, Felsheim R, Dean AM. The biochemical architecture of an ancient
790 adaptive landscape. *Science.* 2005;310: 499–501.
- 791 39. Gong LI, Suchard MA, Bloom JD. Stability-mediated epistasis constrains the evolution of an
792 influenza protein. *Elife.* 2013;2: e00631.
- 793 40. Mobasheri A, Avila J, Cózar-Castellano I, Brownleader MD, Trevan M, Francis MJ, et al.
794 Na⁺, K⁺-ATPase isozyme diversity; comparative biochemistry and physiological
795 implications of novel functional interactions. *Biosci Rep.* 2000;20: 51–91.
- 796 41. Haas BJ, Papanicolaou A, Yassour M, Grabherr M, Blood PD, Bowden J, et al. De novo
797 transcript sequence reconstruction from RNA-seq using the Trinity platform for reference
798 generation and analysis. *Nat Protoc.* 2013;8: 1494–1512.

- 799 42. Darriba D, Posada D, Kozlov AM, Stamatakis A, Morel B, Flouri T. ModelTest-NG: a new and
800 scalable tool for the selection of DNA and protein evolutionary models. *Mol Biol Evol.*
801 2020;37: 291–294.
- 802 43. Stamatakis A. RAxML version 8: a tool for phylogenetic analysis and post-analysis of large
803 phylogenies. *Bioinformatics.* 2014;30: 1312–1313.
- 804 44. Guindon S, Dufayard J-F, Lefort V, Anisimova M, Hordijk W, Gascuel O. New algorithms and
805 methods to estimate maximum-likelihood phylogenies: assessing the performance of
806 PhyML 3.0. *Syst Biol.* 2010;59: 307–321.
- 807 45. Yu G, Smith DK, Zhu H, Guan Y, Lam TT. ggtree: an R package for visualization and
808 annotation of phylogenetic trees with their covariates and other associated data. *Methods*
809 *Ecol Evol.* 2017;8: 28–36.
- 810 46. Yang Z. PAML 4: phylogenetic analysis by maximum likelihood. *Mol Biol Evol.* 2007;24:
811 1586–1591.
- 812 47. Pagel M, Meade A. Bayesian analysis of correlated evolution of discrete characters by
813 reversible-jump Markov chain Monte Carlo. *Am Nat.* 2006;167: 808–825.
- 814 48. Petschenka G, Fandrich S, Sander N, Wagschal V, Boppré M, Dobler S. Stepwise evolution
815 of resistance to toxic cardenolides via genetic substitutions in the Na⁺/K⁺-ATPase of
816 milkweed butterflies (Lepidoptera: Danaini). *Evolution.* 2013;67: 2753–2761.
- 817 49. Taussky HH, Shorr E. A microcolorimetric method for the determination of inorganic
818 phosphorus. *J Biol Chem.* 1953;202: 675–685.
- 819
- 820

821 **Figures and Tables**

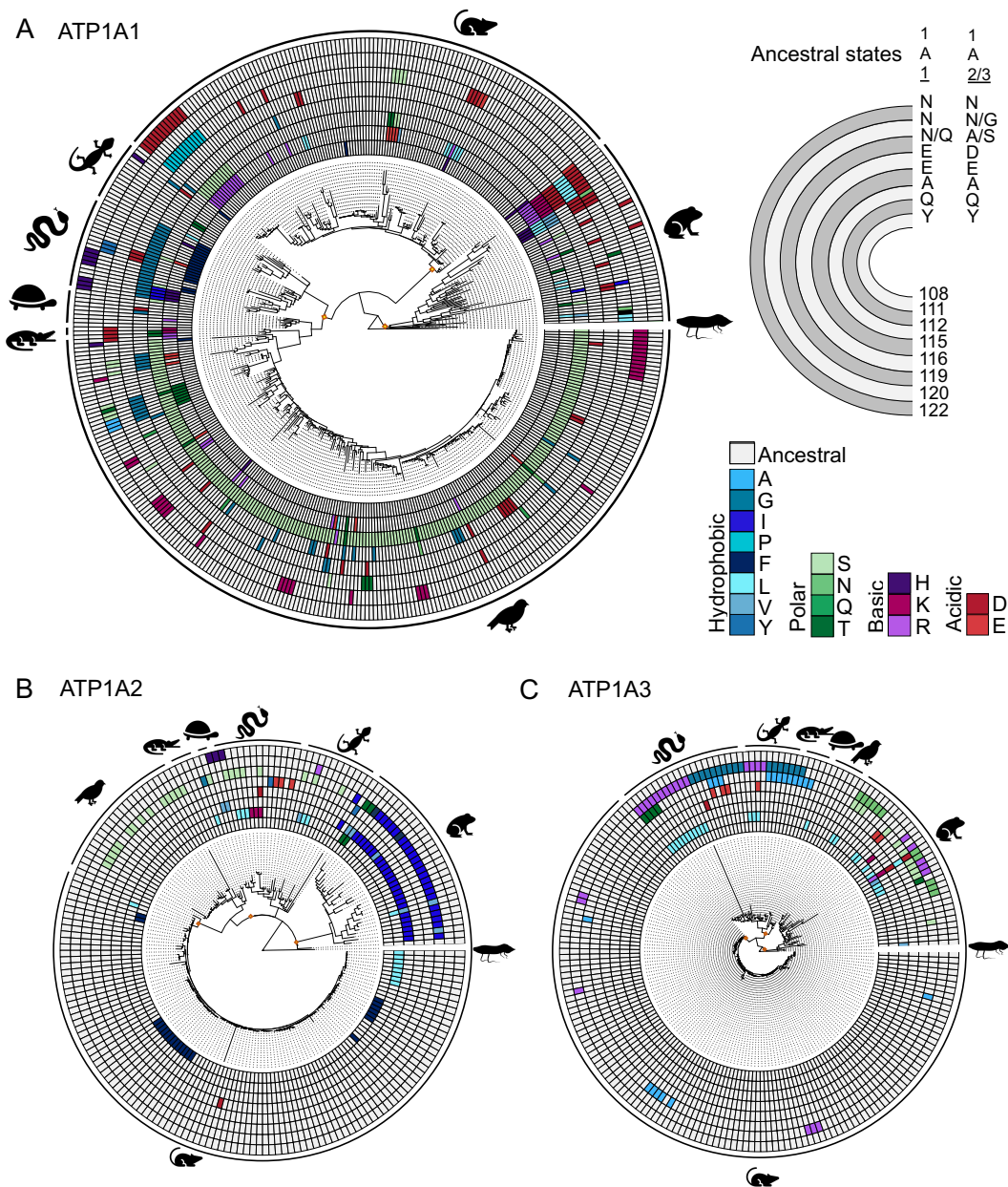
822

823



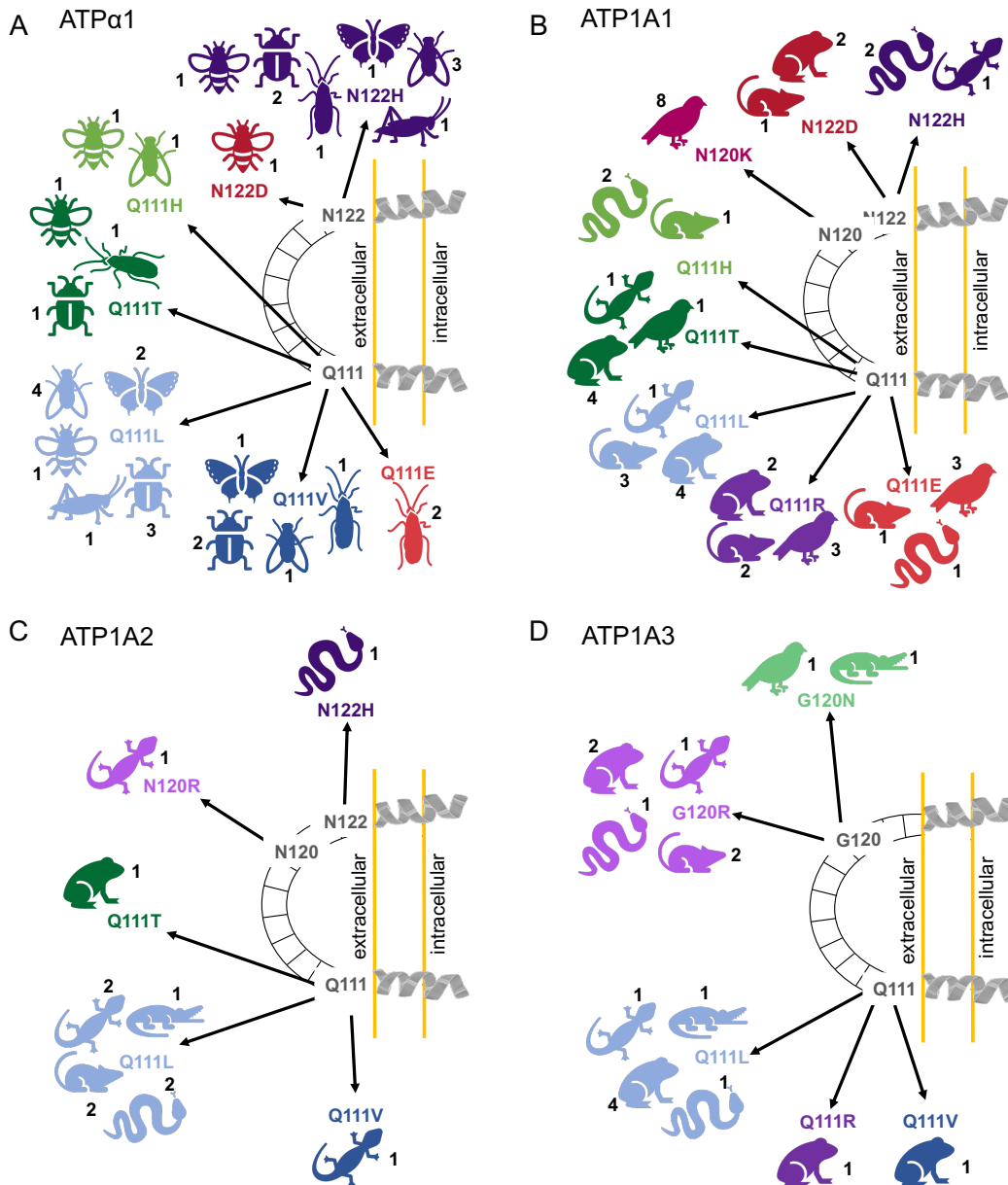
824

825 **Figure 1. Na,K-ATPase structure and phylogenetic relationships of ATP1A paralogs among**
826 **vertebrates.** (A) Crystal structure of an Na⁺,K⁺-ATPase (NKA) with a bound the representative CTS
827 bufalin in blue (PDB 4RES). The zoomed-in panel shows the H1-H2 extracellular loop, highlighting
828 two amino acid positions (111 and 122 in red) that have been implicated repeatedly in CTS
829 resistance. We highlight key examples of convergence in amino acid substitutions at sites in the
830 H1-H2 extracellular loop associated with CTS resistance in Fig. 3. (B) Phylogenetic relationships
831 among ATP1A paralogs of vertebrates and ATP α of insects.
832



833
 834 **Figure 2. Patterns of molecular evolution in the α (H1–H2) extracellular loop of ATP1A**
 835 **paralogs shared among tetrapods.** (A) Maximum likelihood phylogeny of tetrapod ATP1A1, (B)
 836 ATP1A2, and (C) ATP1A3. The character states for eight sites relevant to CTS resistance in and
 837 near the H1-H2 loop of the NKA protein are shown at the node tips. Yellow internal nodes indicate
 838 ancestral sequences reconstructed to infer derived amino acid states across clades to ease
 839 visualization; nodes reconstructed: most recent common ancestor (MRCA) of mammals,
 840 and of amphibians. *Top right*, each semi-circle indicates the site mapped in the main phylogeny
 841 with the inferred ancestral amino acid state for each of the three yellow nodes (posterior probability
 842 >0.8). In ATP1A1, site 119 was inferred as Q119 for amphibians and mammals, and N119 for
 843 reptiles (Table S6); in ATP1A2-3 site 119 was inferred as A119 for amphibians and reptiles,
 844 and S119 for mammals (Table S6). Site number corresponds to pig (*Sus scrofa*) reference sequence.
 845 Higher number and variation of substitutions in ATP1A1 stand out in comparison to the other
 846 paralogs.

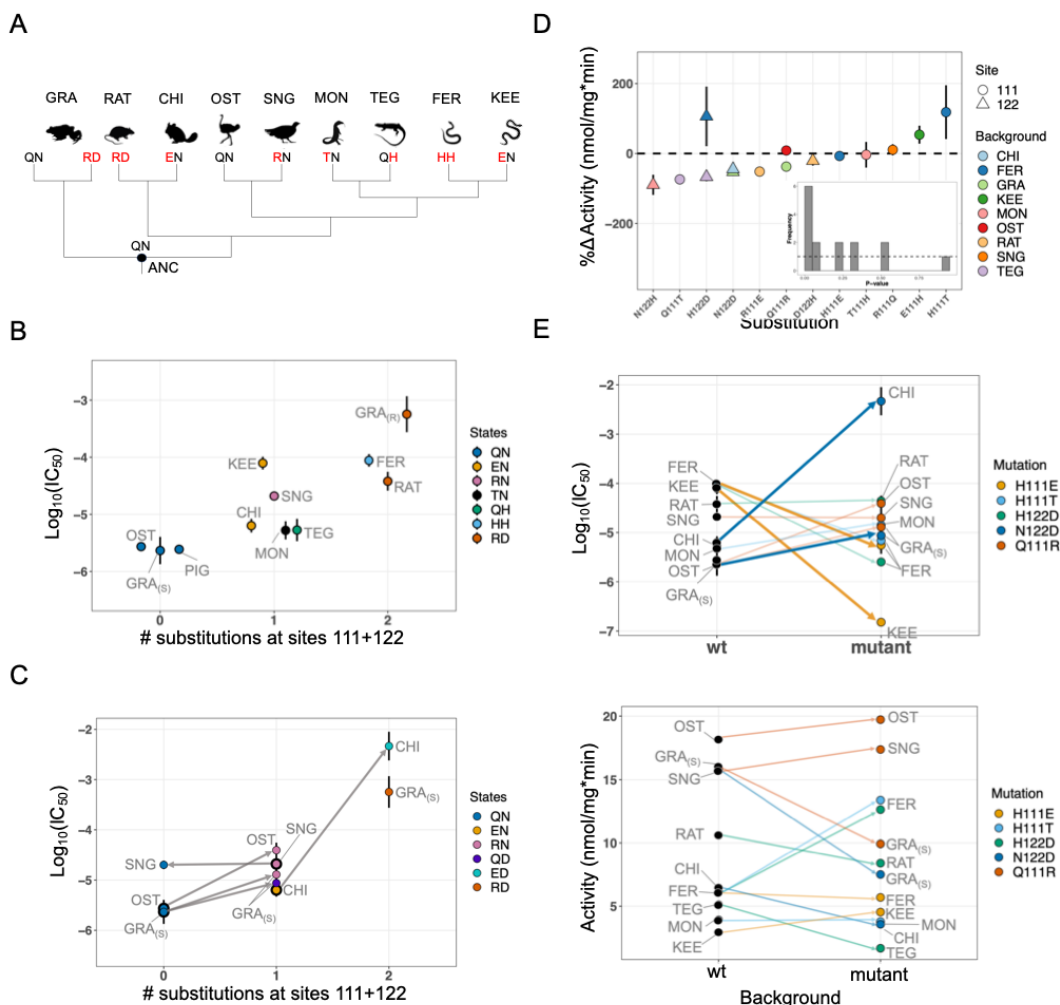
847



848

849

850 **Figure 3. Parallel and divergent patterns of CTS-resistant substitutions across ATPα1 of**
 851 **insects and the shared ATP1A paralogs of tetrapods.** Examples of convergence in ATPα1
 852 across insects (A). Convergence in the (B) ATP1A1, (C) ATP1A2, and (D) ATP1A3 paralogs,
 853 respectively, across tetrapods. Numbers indicate the number of independent substitutions in each
 854 major clade depicted. For ATP1A3, resistance-conferring amino acid substitutions have been
 855 identified at site 120, and not 122. A full list of amino acid substitutions can be found in
 856 Supplementary Dataset 2 for tetrapods, and Taverner et al. [23] for insects.
 857

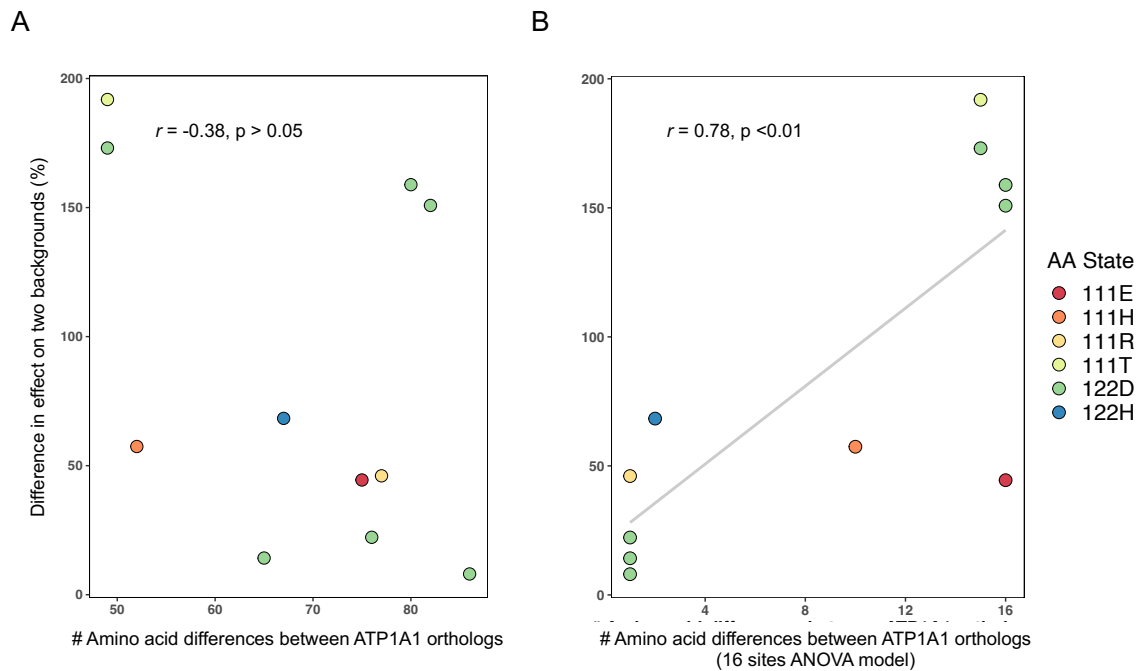


858

859 **Figure 4. Functional properties of wild-type and engineered ATP1A1.** (A) Cladogram relating
 860 the surveyed species. GRA: Grass Frog (*Leptodactylus*); RAT: Rat (*Rattus*); CHI: Chinchilla
 861 (*Chinchilla*); OST: Ostrich (*Struthio*); SNG: Sandgrouse (*Pterocles*); MON: Monitor lizard
 862 (*Varanus*); TEG: Tegu lizard (*Tupinambis*); FER: False fer-de-lance (*Xenodon*); KEE: Red-necked
 863 keelback snake (*Rhabdophis*). Two-letter codes underneath each avatar indicate native amino acid
 864 states at sites 111 and 122, respectively. Data for grass frog from Mohammadi et al. [25]. (B) Levels
 865 of CTS resistance (IC₅₀) among wild-type enzymes. The x-axis distinguishes among ATP1A1 with
 866 0, 1 or 2 derived states at sites 111 and 122. The subscripts S and R refer to the CTS-sensitive
 867 and CTS-resistant paralogs, respectively. (C) Effects on CTS resistance (IC₅₀) of changing the
 868 number of substitutions at 111 or 122. Substitutions result in predictable changes to resistance
 869 except in the reversal R111Q in Sandgrouse (SNG). GRA_S represents Q111R+N122D on the
 870 sensitive paralog background. (D) Effects of single substitutions on Na,K-ATPase (NKA) activity.
 871 Each modified ATP1A1 is compared to the wild-type enzyme for that species. The inset shows the
 872 distribution of *t*-test *p*-values for all 15 substitutions, with the dotted line indicating the expectation.
 873 (E) Evidence for epistasis for CTS resistance (IC₅₀, upper panel) and lack of such effects for
 874 enzyme activity (lower panel). Each line compares the same substitution (or the reverse
 875 substitution) tested on at least two backgrounds. Thicker lines correspond to substitutions with
 876 significant sequence-context dependent effects (Bonferroni-corrected ANOVA *p*-values < 0.05,
 877 Table S5).

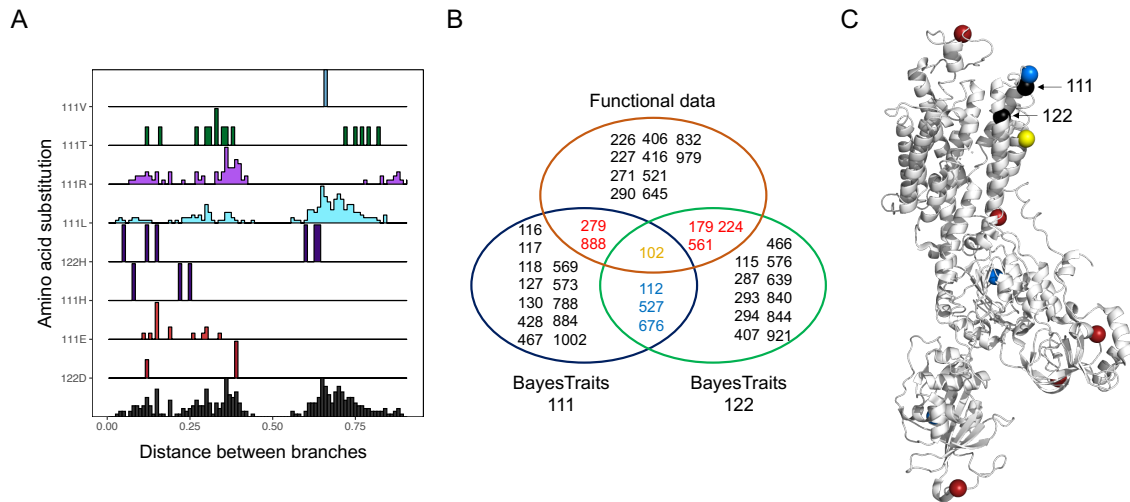
878

879



880

881 **Figure 5. A small number of sites account for a large proportion of the differences in**
882 **pleiotropic effects of the same substitution on divergent backgrounds.** (A) The difference in
883 effect size of a mutation to a given state on two different backgrounds as a function of divergence
884 at all sites. Each point represents a comparison between the effect (% change in activity relative to
885 the wild-type enzyme) of a given amino acid state (e.g., 122D) on two different genetic backgrounds.
886 For example, the effect of 122D between chinchilla and false fer-de-lance is measured as $|\Delta\%$
887 [chinchilla vs. chinchilla+N122D] minus the $\Delta\%$ [false fer-de-lance vs. false fer-de-lance+H122D]].
888 Comparisons were measured as the difference between the two effects. The x-axis represents the
889 number of amino acid differences between two wild-type ATP1A1 proteins (i.e., backgrounds) being
890 compared. Assuming intramolecular epistasis for protein function is prevalent, a positive correlation
891 is predicted. In total, 11 comparisons were possible, and no significant correlation is observed when
892 considering divergence at all sites. (B) The difference in effect size of a mutation to a given state
893 on two different backgrounds as a function of divergence at a subset of 16 sites with the largest
894 effects on the difference in activity between two backgrounds. The p-value of the correlation was
895 determined by permuting effects among constructs and generating a null distribution of correlations.
896



897

898 **Figure 6.** (A) Distribution of amino acid substitutions at sites 111 and 122 across all paralogs. For
 899 each derived amino acid state at sites 111 and 122, the histograms show the distribution of pairwise
 900 convergent events along the sequence divergence axis (expected number of substitutions per site).
 901 Substitutions are color coded as in Fig. 2. The histogram at the bottom shows the combined
 902 distribution of pairwise convergent events for both sites. (B) Intersection of 16 sites identified from
 903 functional data with the sites that most strongly correlated with substitutions at sites 111 and 122
 904 Sites in the “functional data” group correspond to the 16 sites from the two groups identified by the
 905 ANOVA model (Tables S8 and S9). Sites in the BayesTraits analyses groups correspond to the top
 906 5% sites with highest $-\log(P)$ association with 111 or 122, respectively. Overlaps between each
 907 group are larger than expected by chance: $\text{Functional} \cap \text{BayesTraits}_{111} = 3$, $P = 0.049$; $\text{Functional} \cap$
 908 $\text{BayesTraits}_{122} = 4$, $P = 0.007$; $\text{BayesTraits}_{111} \cap \text{BayesTraits}_{122} = 4$, $P = 0.011$. (C) Crystal
 909 structure of ATP1A1 (PDB 3B8E) showing sites color coded according to the intersections in panel
 910 B.